Overview of the Ground-to-Orbit Lasercom Demonstration

K. E. Wilson and J. R. Lesh,
Jet Propulsion Laboratory
California Institute of Technology
Pasadena, California 91101

Abstract

The Ground-to-Orbit Lasercom Demonstration conducted between the ETS-VI spacecraft and the ground station at JPL's Table Mountain Facility, Wrightwood CA was the first ground-to-space two-way optical communications experiment. The demonstration was conducted over a period of seven months and required simultaneous and cooperative operations by team members in Tokyo and California. A key objective was to measure the atmospheric attenuation and seeing during the demonstration to evaluate the performance of the optical link. The optical downlink telemetry provided information on the in-orbit performance of ETS-VI's laser communications equipment. Downlinked PN data enabled measurement of hit error rates. BERs as low as 10^{-4} were measured on the uplink and 10"5 on the downlink. Measured signal powers (corrected for measured atmospheric attenuation) agreed with theoretical predictions.

1. Introduction

More sophisticated space-borne science instruments have increased the demand for higher data rates, a demand that is not envisioned to be met by the bandwidth-limited rf spectrum. The launch of the ETS-VI satellite with its on-board laser communications equipment (LCE) opened a new chapter in satellite communications[1]. Optical communications offers extremely high data rate communications from LEO and GEO satellites without spectrum allocations and bandwidth restrictions. The failure of the ETS-VI's apogee kick motor prevented the satellite from achieving geostationary orbit and left it in an elliptical geo-transfer orbit. In this orbit the satellite was visible from ground stations around the world. The Communications Research Laboratory asked NASA/JPL to participate in a Ground-to-Orbit Lasercom Demonstration (GOLD) optical communications demonstration with the ETS-VI. NASDA modified the satellite's orbit to improve it for the TMF demonstration and carefully monitored its power consumption to maximize the lasercom demonstration opportunity.

The GOLD experiments were performed over the seven month period extending from October 1995 to May 1996 [2]. There were two transmissions phases separated by an apogee eclipse phase that lasted from mid-January to mid-March. The Jet Propulsion Laboratory (JPL) and Communications Research Lab (CRL) GOLD teams negotiated the transmission opportunities with the DSN (Deep Space Network) and NASDA (National Aeronautics and Space Development Agency). Laser transmissions occurred every third day as the satellite's orbit brought it to apogee over Table Mountain Facility (TMF). Transmissions lasted for a period of three to five hours and ranged from very early-morning hours during Phase- 1 to mid-afternoon passes towards the end of Phase-2.

An internationally cooperative demonstration, GOLD required the simultaneous real-time coordination of experimenters at NASDA, CRL, the DSN, JPL, and TMF. The command and data flow diagram is shown in Figure 1. Approximately two hours before the scheduled uplink NASDA began to adjust the satellite's attitude to ensure that the ground station would be within the laser communications equipment (LCE's) field of view during

the pass over TMF. Commands were transmitted from NASDA to the DSN'S DSS-27 antenna at Goldstone. Approximately 30 minutes before transmission, CRL began to issue commands via NASDA to turn on the LCE. With the satellite oriented and the LCE ready to receive the uplink, laser transmission was initiated from TMF. On most occasions the uplink was detected by the satellite and the downlink was subsequently received at TMF. The times when it was not, the LCE and the ground station operators alternately scanned the uplink beam and the LCE's coarse pointing gimbal until the link was established.

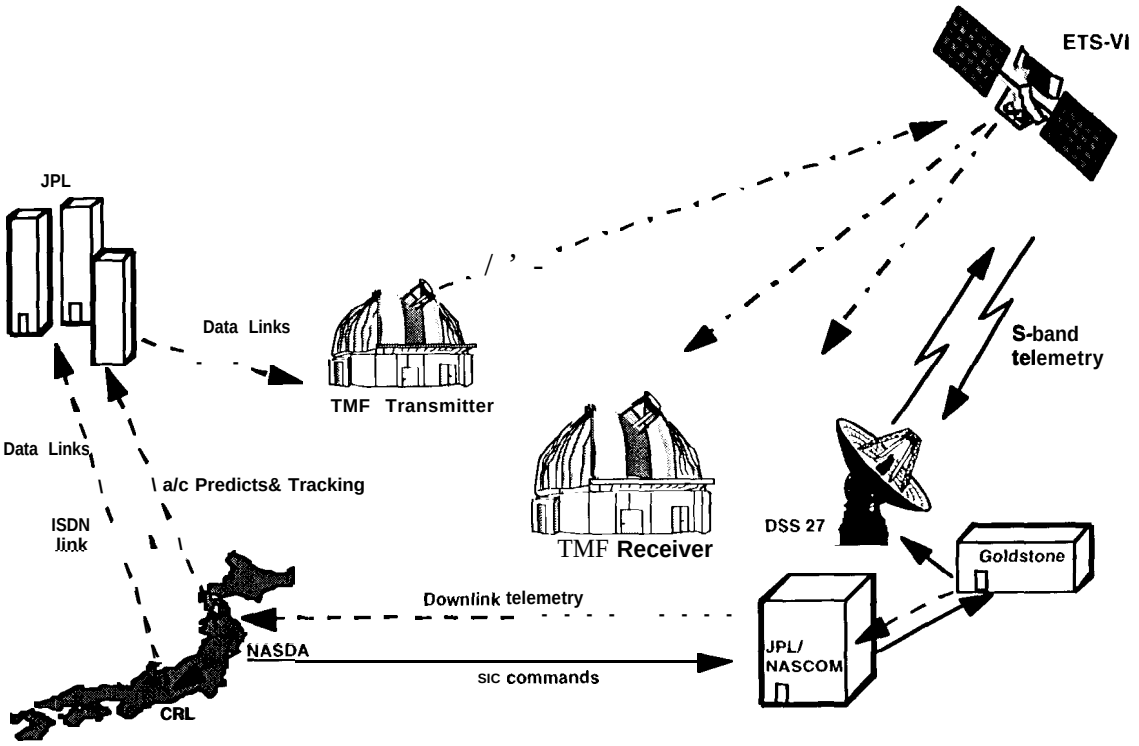

Figure 1: Real time coordination of several organizations was needed to accomplish the GOLD experiment. NASDA transferred commands to the DSN which uplinked them to the ETS-VI. The spacecraft attitude and LCE sensor status were downlinked via S-band telemetry to Goldstone. The telemetry was demodulated by NASDA and forwarded to CRL for processing. During the optical uplink CRL transmitted LCE sensor data to JPL and on to TMF.

This paper presents some of the results of the GOLD demonstration. In Section 2 we discuss the GOLD transmission record over the demonstration and describe the multi -beam uplink in Section 3. This is followed by a discussion of the downlink data record in Section 4 and by our atmospheric measurements in Section 5. Conclusions and references are given in Sections 6 and 7, respectively.

2. GOLD Transmission Record

There were 44 total opportunities to transmit to the satellite, 22 in each of the two GOLD demonstration phases. The pie charts in figures 2.1 and 2.2 give a breakdown of the transmission results during those opportunities. Phase- 1 transmissions extended from

October 30 to January 13 [3]. There were twelve 2-way transmissions, one 1-way transmission, five cancellations due to bad weather, two cancellations due to hardware failures, and two non-detections. The two non-detection events occurred on the first two transmission days of the program and were used to develop strategies for the remaining passes. Phase-2 transmissions began on March 21, 1996 shortly after the satellite had emerged from the apogee eclipse and extended to May 26. During Phase-2, there were twelve successful 2-way transmissions, three one-way transmissions, one non-detection, two cancellations due to bad weather, and three cancellations due to satellite attitude control problems.

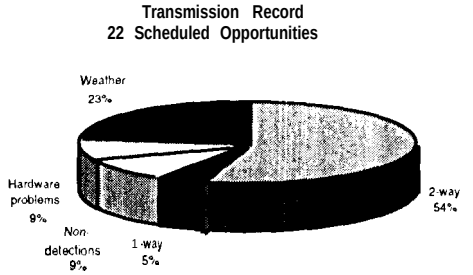

Figure 2.1: Pie chart of GOLD phase-l transmission record Ott, 30 '95 - Jan 13 '96. The nor~-detections occurred on the first two transmission opportunities as satellite and ground station pointing strategies were being exercised. One-way transmission was detection of the uplink signal.

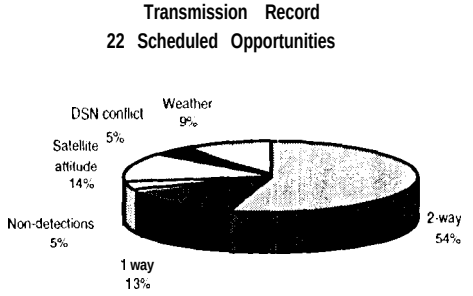

Figure 2.2: Pie chart of GOLD phase-2 transmission record Mar 21, '96 - May 26 '96. The non-detections were due to the loss of the servo loop control and to the inability of the LCE to point to the ground station when the satellite was in the fixed bias mode and ground station pointing strategies were being exercised.

3. Uplink signal detection

Multi-beam propagation was used to mitigate the effects of atmospheric scintillation on the uplink beam. Phase-1 results showed that the uplink scintillation was reduced when two spatially and temporal] y incoherent beams were transmitted to the satellite [4]. In phase-2 the number of beams was increased to four and we measured a further reduction in uplink signal variance.

Over the course of the demonstration we uplinked both an unmodulated beacon and a 1.024 Mbps Manchester coded, 511-bit long PN sequence to the satellite. The modulated uplink allowed us to measure the bit-error rate (BER) on the uplink with multi--beam propagation. Measurements were made using the onboard bit error rate tester (BERT) that counted the number of errors in a one second interval. Init iat ion of the test interval was marked by transmitting a symbol sequence of ones to the satellite that was then followed by the PN transmission. The measured BERs were relayed to the ground on the S-band downlink telemetry. The results of nine such one second measurements are given in Table 1. The measurements were made with a two-beam uplink over a forty minute period on

January 4. The table shows uplink bit error rates on the order of 1 0^{-3} and 10-4. The measured mean atmospheric seeing for the night was measured at 2 arc seconds.

Table 1: Bit-error Rate Measured by LCE on 1 Mbps Uplink

Time	BER
20:10:17	2.49E-03
20:13:55	2.28e-03
20:13:56	2.49e-03
20:18:11	1. 19C-03
20:18:12	2.49e-03
10:36:49	8.01e-04
20:36:50	2.49e-03
20:52:19	3.61e-04
20:52:20	2.49e-03

4. Downlink Signal Recovery

The ground receiver electronics consisted of an APD (avalanche photodiode) coupled to a 3.8 MHz preamplifier circuit [5]. After the preamplifier, the APD signal was divided with one part bit synchronized and then stored on an Exabyte storage tape. The other signal was squared to measure the downlink signal power. We sampled the squared signal at 22 kHz and displayed it on a computer screen. We used scaling factors obtained during the detector calibration measurements to convert the sampled signal to optical power. This gave us a real-time display of the downlink signal power during the experiment. We used these data to guide the CRL team during the process of optimizing the downlink beam pointing.

Figure 4.1 is a plot of the measured and a priori predicted signal strengths. As the figure

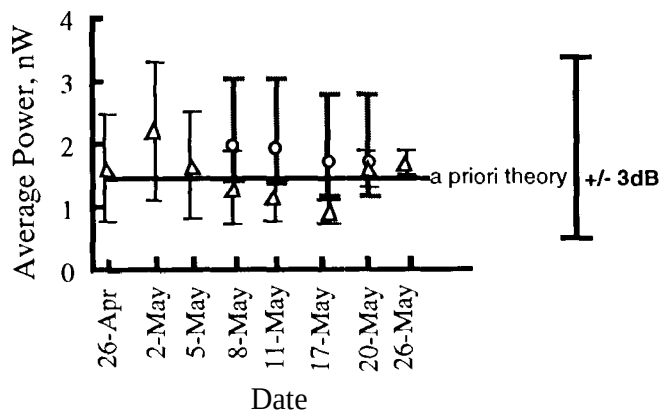

Figure 4.1: Comparison of theoretical prediction and measurement of downlink signal power at 1,2-m receiver. The triangles arc the measured values and the circles arc the theoretical prediction corrected for the measured atmospheric transmission. The error bars arc the standard deviation in the measured power over the course of the experiment.

shows the measured downlink signal strength was within the ± 3 dB uncertainty of the a-priori theory. Our a-priori assumptions were 60 % atmospheric transmission and 5

microradians pointing uncertainty. The error bars on the measured data (measured data depicted by triangles) represent the standard deviation in the measured downlink signal strength. The circles in the figure are the corrected theoretical values based on the measured (not a-priori assumed) value of atmospheric transmission as measured by the autonomous visibility monitoring station at TMF.

There were three operating modes for the downlink optical transmission. These were: (i) a 511 bit-long, 1.024 Mbps pseudo-random (PN) sequence, (ii) 128 kbps LCE telemetry with each bit repeated 8 times to produce a 1.024 Mbps symbol rate (designated E2 data), and (iii) regeneration of a 1.024 Mbps uplink data sequence. Switching between downlink telemetry modes was accomplished in a few seconds. The spectra for the three modes were quite distinct and the switch from one mode to another was readily monitored by using the spectrum analyzer feature of the DSA 602A oscilloscope, To speed up our post-detection data processing we performed FFTs on large blocks of the 22 kHz sampled data to identify the intervals when a specific downlink mode, PN or E2 data was transmitted. This enabled us to go directly to the corresponding data segments stored on magnetic Exabyte tapes.

Figures 4.2 and 4.3 are Fast Fourier Transforms (FFT) of the downlink power fluctuation measured using the APD squaring circuit. The spectra represent an average over fifty minutes of downlink transmission. In both figures the power spectrum rolls off around 10 kHz consistent with the Nyquist criteria for a 22 kHz sampling rate. Figure 4.2 is the FFT of the E2 data stream. It shows a distinct peak at 8 kHz, the frequency of an overlayed amplitude modulation that was impressed by the LCE on the optical downlink. Also evident are the spectral peaks at 500 Hz intervals corresponding to the 2 millisecond-long E2 frame of 2048 bits [6].

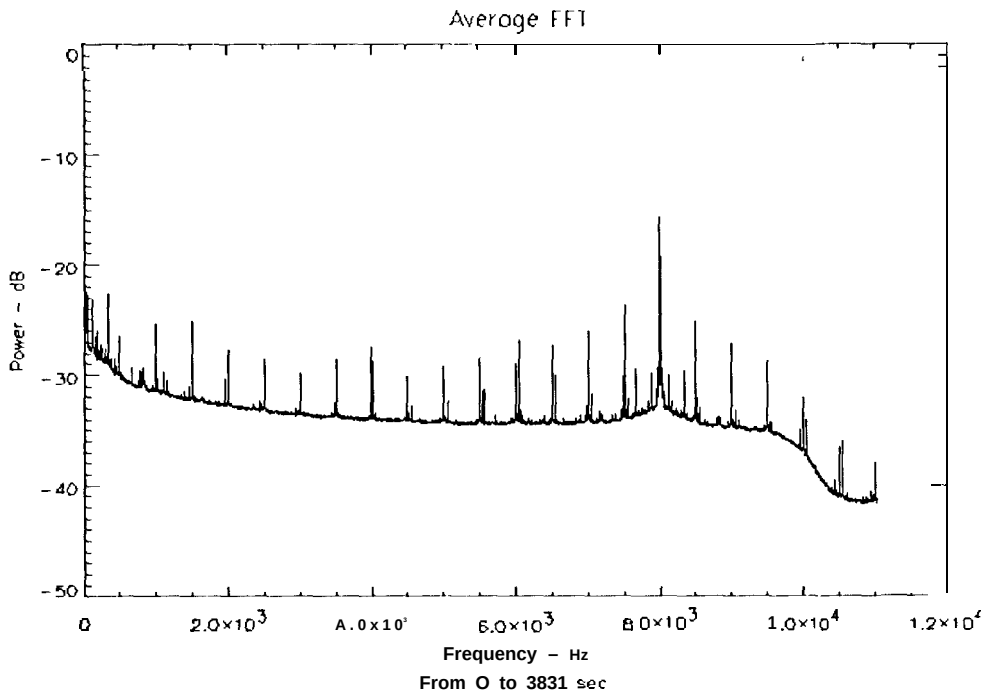

Figure 4.2: FFT of E2 data stream recovered on May 11, 1996. Figure shows the spectral peaks at 500 Hz intervals corresponding to the 2 ms-long E2 data frame.

Figure 43 is a FFT of the received downlink PN data stream. It shows spectral peaks at 2 kHz intervals. This corresponds to the 2.004 kHz repetition frequency of the 511 bit-long

PN sequence in the 1.024 Mbps data stream. Again the figure shows the strong peak at 8 kHz. This is the superposition of the harmonics of the PN spectrum and the 8 kHz amplitude modulation.

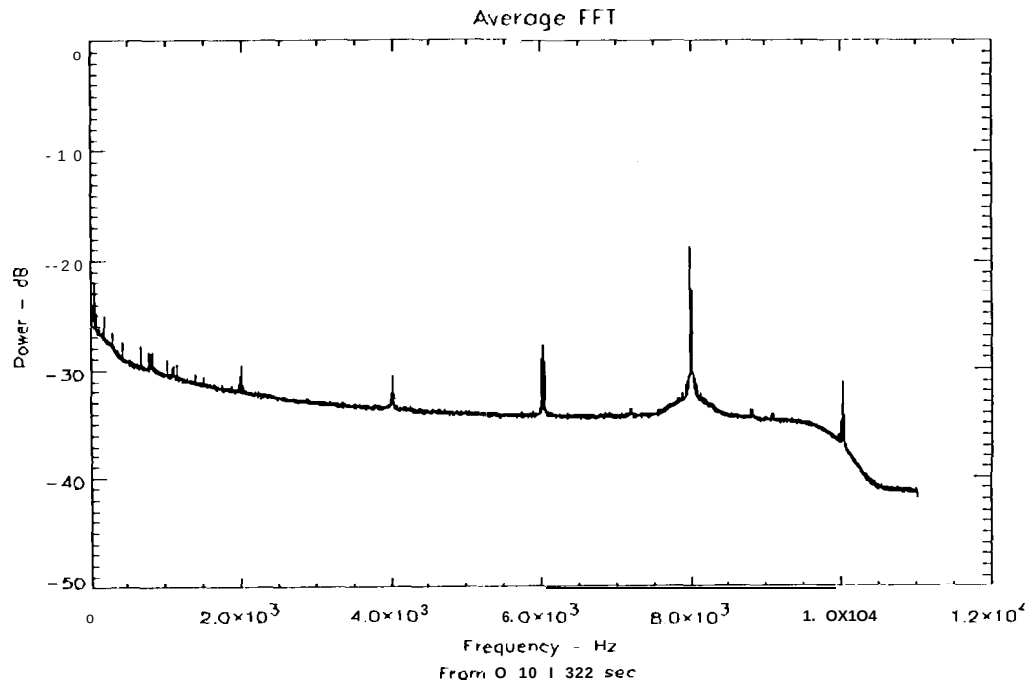

Figure 4.3: FFT of PN downlink data recovered on May 17, 1996. Figure shows 2 kHz interval spectrum corresponding to the 2.004 kHz repetition frequency of the 511 bit-long PN sequence in the 1.024 Mbps data stream. The strong peak at 8 kHz is the superposition of the PN spectrum anti the 8 kHz amplitude modulation of the laser power that was impressed on the optical downlink.

Figure 4.4 shows a plot of the measured downlink BER during the pass of April 27. BER data varied from pass to pass due to a variety of spacecraft, ground and atmospheric conditions, so this plot does not represent performance achieved on all experiment passes. However, it does show that low BERs were obtained from time to time. The figure shows a three-minute-long segment of the downlink BER measurements that were demodulated from the PN data stream. Each data point represents 200 frames or a 100 milliseconds segment of data. The figure shows that the bit errors occur in bursts, and that several frames were error-free (i.e. BERs as low as 10-').

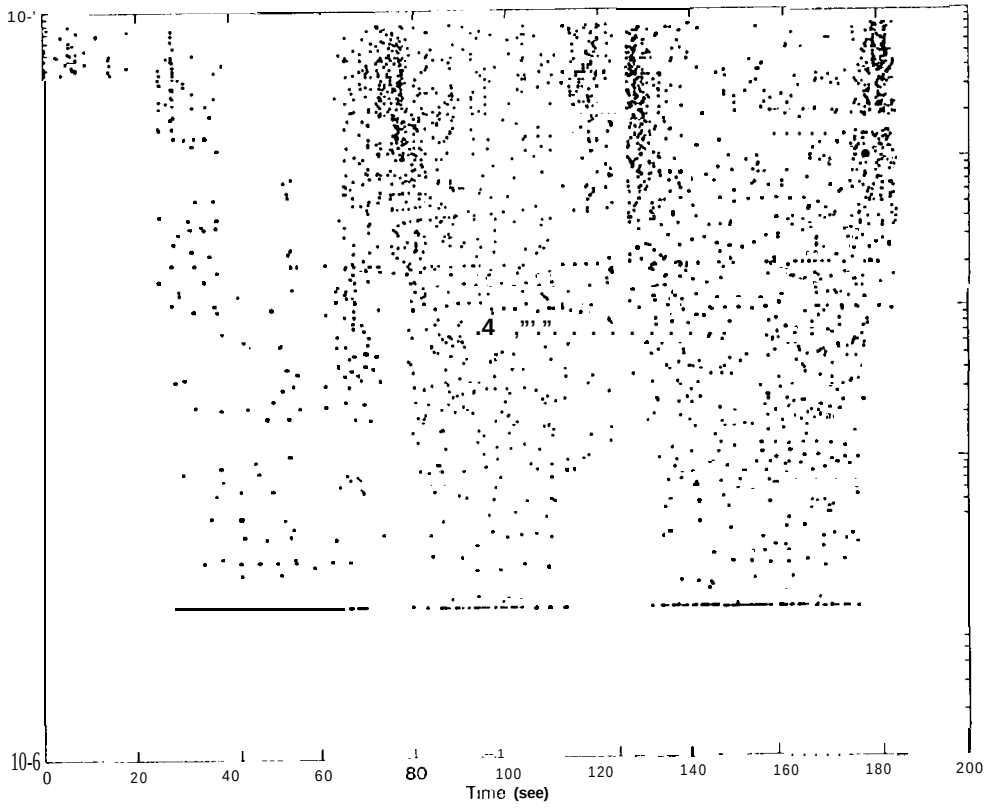

Figure 4.4: Bit Error rate measured in a three-minute-long PN data sequence on April 27, 1996. Each point represents 0.1 seconds of data at 1.024 Mbps.

5. **Atmospheric Seeing Measurements**

Figures 5.1 and 5.2 show the atmospheric seeing measurements recorded during the GOLD experiment. Atmospheric turbulence caused by temperature and pressure variations in the atmosphere results in scintillation of the light from a point-source as it propagates through the atmosphere. On the downlink, this effect is averaged out over large ground receiving apertures [7]. On the uplink, however, turbulence causes both scintillation and beam wander (tilt) in a laser beam transmitted from a ground station to a space-borne receiver. These effects, if left uncompensated are manifested as fades and surges in the uplink signal, resulting in high bit errors in the uplink communications data stream.

Seeing measurements were made at 15 minute intervals from the TMF 1.2-m receiver telescope using a Spectra Source slow scan CCD camera with a software package designed for this purpose. The CCD camera was coaligned with the APD and the detected downlink signal was integrated for several seconds. The atmospheric seeing was determined from the full-width-at-half-maximum of the measured intensity distribution on the CCD array.

Signal to several seconds so as to allow the CCD camera to

have predicted the advantages of multi-beam transmission over that of a single beam and these were verified by the experiment.

Acknowledgments

The authors would like to recognize the contributions of the other GOLD team members at the CRL, NASDA, the DSN and at JPL for their dedication to this demonstration.

The research described in this paper was carried out at the Jet Propulsion Laboratory, California Institute of Technology, under a contract with the National Aeronautics and Space Administration.

References

1. M. Shikatani et al. "Ground System Development for the ETS-VI/LCE Laser Communications Experiment" SPIE Proceedings vol. 1866, Jan. 1993, Los Angeles, CA.
2. K. E. Wilson, M. Jeganathan, J. James, G. Xu and J. R. Lesh, "Results From Phase- 1 and Phase-2 GOLD Experiments" JPL TDA Progress Report 42-127, November 151996.
3. K. E. Wilson, "Preliminary Results, Analysis and Overview of Part-1 of the GOLD Experiment", Invited Paper, CRL International Symposium on Advanced Technologies in Optical Communications and Sensing, Tokyo, March 13, 1996.
4. M. Jeganathan, K. Wilson, J. R. Lesh, "Preliminary analysis of Fluctuations in Received Uplink Beacon Power Data Obtained from GOLD Experiments", JPL TDA Report 42-124, February 15.1996.
5. C. Pasqualino "Characterization of the Avalanche Photodiode detector used for Optical Communications Experiments with the Japanese ETS-VI Satellite" JPL TDA Progress Report 42-127.
6. M. Toyoshima, M. Jeganathan et al. "Reduction of ETS-VI/LCE Optical Downlink Telemetry Collected During GOLD', JPL TDA Progress Report 42-127.
7. K. E. Wilson, A. Biswas, S. Bloom, and V. Chan "Effect of Aperture Averaging on a 570 Mbps 42 km Horizontal Path Optical Link", SPIE Proceedings vol. 2471, April 1995, Orlando FL.